# Laser pulse propagation in a meter scale rubidium vapor/plasma cell in AWAKE experiment

A. Joulaei<sup>1, 3</sup>, J.Moody<sup>1</sup>, N. Berti<sup>2</sup>, J. Kasparian<sup>2</sup>, S. Mirzanejhad<sup>3</sup> and P. Muggli<sup>1</sup>

Max-Planck Institute for Physics, Munich, Germany,
<sup>2</sup>University of Geneva, Switzerland,
<sup>3</sup>Uiversity of Mazandaran, Iran.

# November 2015

### **Abstract**

We present the results of numerical studies of laser pulse propagating in a 3.5 cm Rb vapor cell in the linear dispersion regime by using a 1D model and a 2D code that has been modified for our special case. The 2D simulation finally aimed at finding laser beam parameters suitable to make the Rb vapor fully ionized to obtain a uniform, 10 m-long, at least 1 mm in radius plasma in the next step for the AWAKE experiment.

### I. Introduction

AWAKE is a proof-of-principle proton-driven plasma wakefield electron acceleration experiment at CERN [1, 2]. The purpose of the experiment is to understand the physics of the acceleration process to demonstrate high-gradient acceleration of electrons from MeV to GeV energy scale within a 10 meter plasma with an electron density of  $10^{14} - 10^{15} \text{ cm}^{-3}$  and driven by a proton bunch. The experimental program is based on the numerical simulations of the beam and plasma interaction. An ultrashort terawatt Gaussian laser pulse ionizes a rubidium (Rb) vapor in a 10 m long vapor/plasma cell, creating plasma that acts as an energy transformer from the proton drive bunch to the electron witness bunch that accelerates. It also seeds the self-modulation instability with a sharp, moving ionization front. To mitigate the effects of plasma density ramps at the entrance and exit of the plasma, limiting apertures have been proposed. The minimum aperture radius is limited by diffraction of the laser pulse when

crossing the entrance one. Also, along propagation of the laser pulse in the gas/vapor to ionize and in the plasma, dispersion, kerrinduced self-focusing and filamentation may occur. These effects potentially lead to a decrease in laser pulse intensity below the rubidium ionization threshold, thereby limiting the radial and longitudinal extent of the plasma. Some of these effects may be particularly important when the laser pulse spectrum overlaps with an atomic transition of the medium to ionize and the pulse experiences anomalous dispersion effects, as in the AWAKE Rb vapor case.

For the AWAKE experiment, the propagation of the laser pulse intensity is simulated by using a 2D code [3, 4]. We initially test the code in the low intensity regime of laser pulse and compare results between 1D calculations, results of the 2D code and also with experimental results. To ensure the code accuracy in the high-intensity laser regime, full ionization of the vapor and plasma creation

In this paper, we present results of numeri-

cal studies of laser pulse intensity after propagation in a 3.5 cm-long Rb vapor cell in linear regime.

### II. SIMULATIONS

The laser pulse interaction with the Rb vapor is simulated with a code that is typically used to model the ionizing laser propagation through the atmosphere [4]. The code is 2D with cylindrical coordinate (r,z). It solves the master paraxial propagation equation:

$$\nabla^2 E - \frac{1}{c^2} \partial_t^2 E = \mu_0 (\partial_t J + \partial_t^2 P). \tag{1}$$

Here E is the laser pulse electric field profile, J is the current and P is the polarization, including the linear and nonlinear response of the medium. The polarization is written in orders of E as:

$$P(t) = \varepsilon_0(\chi^1 E(t) + \chi^2 E^2(t) + \dots).$$
 (2)

The coefficients  $\chi^n$  are the n-th order susceptibilities of the medium and the presence of such a term is generally referred to as an n-th order non-linearity. Typically, Equation 1 is solved also to all orders in the 2D code by using the Fourier transform split step method. The equation is solved in the frequency and wave number domain and a unitary transformation (phase shift transformation) is applied with the resulting longitudinal wavenumber  $k_z$ . This transformation is responsible for diffractive and linear dispersion effects. In this method the linear dispersion and diffraction effects are applied in the frequency and wave number domains. We use the Hankel-Fourier transform:

$$F(k) = \int_{r=0}^{\infty} \int_{\theta=0}^{2\pi} f(r,\theta) e^{ikr\cos(\theta)} r dr d\theta.$$
 (3)

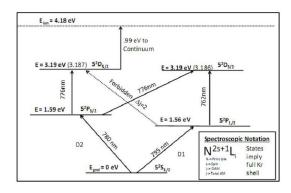
when cylindrical symmetry applied to this, it becomes:

$$F(k) = \int \int f(r,\theta)e^{ik.r}rdrd\theta$$
$$= 2\pi \int_0^\infty f(r)J_0(kr)rdr. \quad (4)$$

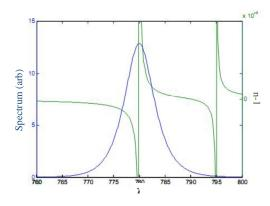
Its inverse is:

$$f(r) = \frac{1}{(2\pi)^2} \int F(k)e^{-ik.r}dk = \frac{1}{2\pi} \int_0^\infty F(k)J_0(kr)rdr.$$
 (5)

The Hankel-Fourier transform of order zero is essentially the 2-dimensional Fourier transform of a circularly symmetric function. The code changes between the frequency and time domains. The laser pulse is implemented in the time domain in order to apply intensity dependent effects and the nonlinear polarization terms as well as ionization losses and kerr effect.

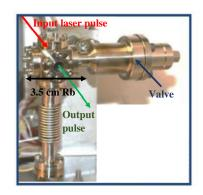


**Figure 1:** *Diagram of Rb valence electronic state* [5].



**Figure 2:** Laser spectrum (blue line) and real part of the refractive index (green line) of Rb near the D2 optical transition line from the ground state with density  $6 \times 10^{14}$  cm<sup>-3</sup>.

# III. Methods



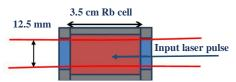


Figure 3: Scheme of the 3.5 cm Rb source

The linear interaction between light at frequency  $\omega_0$  with the medium with atomic absorption lines at  $\omega_{ij}$  is described by the linear susceptibility Equation 6 [6]:

$$\chi^{1}(\omega) = \sum_{i} \frac{N_{i}e^{2}}{\varepsilon_{0}m_{e}} \sum_{j} \frac{f_{ij}}{\omega_{ij}^{2} - \omega_{0}^{2} + i\Gamma_{i}\omega_{ij}}.$$
 (6)

The coefficients  $\chi^1$  is the linear susceptibility,  $N_i$  the atomic density, e the electron charge,  $\varepsilon_0$  vacuum permittivity,  $m_e$  is the electron mass,  $f_{ij}$  absorption oscillator strength,  $\omega_{ij}$  is the absorption line of vapor,  $\omega_0$  central laser frequency and  $\Gamma_i$  is the transition life time. This parameter describes the linear polarization as the linear response of the medium since:

$$P^{1}(t) = \varepsilon_0 \chi^{1} E(t). \tag{7}$$

Based on the two equations below the refractive index and wave vector are also calculated in the frequency domain of the 2D code:

$$n_1(\omega) = \sqrt{1 + \chi^1(\omega)}.$$
 (8)

$$k(\omega) = n(\omega) \frac{\omega}{c}.$$
 (9)

The laser used in the experiment is an Erbiumdoped fiber oscillator with a central wavelength of 780 nm and a bandwidth of approximately 10 nm. The laser is a chirped pulse amplification system that stretches the  $\sim 100$ fs pulse to  $\sim 100$  ps, amplifies it to a maximum energy of 600 mJ, then recompresses it to a peak power of  $\sim 4$  TW at a maximum energy of 450 mJ. The plasma is produced from a  $1-10^{15}~cm^{-3}$  rubidium vapor source. Rubidium was chosen over other alkali metals because of its low ionization potential of 4.2 eV and the relative technical simplicity of its use, including producing the baseline vapor density at 200 °C. It is also solid at room temperature [7]. To create the plasma, the rubidium is photo-ionized by multiphoton ionization (AC field ionization) described by the Keldysh parameter [8, 10]. Because we are operating in a low Keldysh parameter regime in which the intensity is high and frequency low, the ionization time is much less than the laser pulse length and occurs at a laser threshold intensity of  $\sim 2 \text{ TW/cm}^2$ .

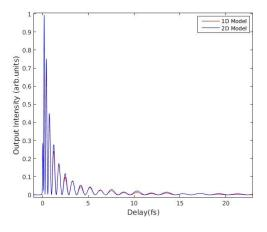
We use a small rubidium cell with a length of 3.5 cm and the diameter of 12.5 mm and a vapor density of  $6 \times 10^{14}$  cm<sup>-3</sup>. Upon verification of the rubidium vapor density for a given temperature,  $400~\mu J$  of laser pulses with the pulse width FWHM of 100 fs and an average intensity of  $1~GW/cm^2$  is propagated through the cell. In this low intensity regime the vapor ionization is negligible.

Figure 1 shows some of the atomic transitions of the Rb atom. In patricular, Rb has a transition (known as D2) from the ground states at 780.241 nm that falls near the peak of the laser pulse spectrum. Figure 2 shows the anomalous dispersion in the vicinity of this line calculated using Equation 6. This anomalous dispersion can stretch the laser pulse.

# IV. RESULT AND ANALYSIS

The length of the laser pulse is determined with a second harmonic generation intensity autocorrelator . As a background, the pulse length is measured through the cell at room temperature (no Rb) and as expected, there is negligible pulse stretching through the cold cell. This can be seen from autocorrelation data of the experiment that is shown on Figure 5. The same figure shows that over the 3.5 cm cell with Rb density of  $6\times 10^{14}~cm^{-3}$  the pulse stretches dramatically with the pedestal increasing in amplitude by a factor of 5.

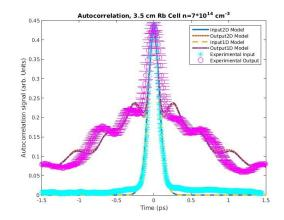
Figure 4 shows the laser pulse intensity simulation from the 1D model and 2D code after propagation through the 3.5 cm Rb cell. The models are consistent with each other and the two dimensional numerical effects are small.



**Figure 4:** Propagated laser pulse intensity simulation in 1D model and 2D code.

Figure 5 compares the laser pulse intensity autocorrelation of the models with that of the experimental measurement. The error estimates represented by the error bars were computed by taking the standard deviation several autocorrelation samples divided by  $\sqrt{N}$ , where N was the number of samples we took at a given temperature. The computed autocorrelation of the models and that of the measurement are consistent with each other despite the models using a simplified spectrum and ignoring any nonlinear effects. Some of the nonlinear

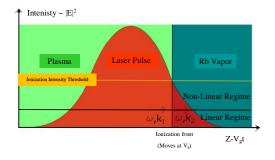
effects are apparent in Figure 7. Frequency dependent Kerr effect is most likely responsible for some of the spectral change, and a near-resonance frequency dependent Kerr model is currently under development.



**Figure 5:** Laser pulse intensity autocorrelation simulation in 1D model, 2D code and experimental measurement.

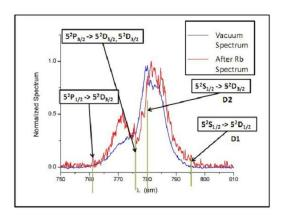
The 2D intensity simulation result and its auto correlation are consistent with the 1D model and experimental results that shows laser pulse stretching in the linear regime.

Figure 1 shows that Rb has two absorption lines at 780.241 and 794.979 nm from its ground state (see Figure 7). Since these two lines are within the incoming laser pulse spectrum, strong excitation of electrons to the upper states of these transitions is expected.



**Figure 6:** *High intensity laser pulse.* 

When the laser intensity is low, its interaction with the Rb vapor is the linear regime. In this case the input and output laser spectra are the same. At higher laser pulse intensities the interaction becomes nonlinear and the spectrum of laser pulse after the Rb vapor is expected to change.



**Figure 7:** Expertimenral input and output spectrum through the 3.5 cm cell at Rb target with the Density  $n \sim 10^{15}$  cm<sup>-3</sup>,  $I \sim 1$  GW/cm<sup>2</sup>.

For the AWAKE experiments the Rb vapor must be fully ionized (first electron) to transform the very uniform neutral Rb density into a very uniform plasma density. However, the laser pulse starts at low intensity and rises to above the ionization intensity with its  $\sim$ 100 fs length (see Figure 6). Therefore, various time slices of the laser pulse interact with the Rb vapor in various regimes. The very front, at low intensity (as described above) interacts in the linear regime. Other than narrow band absorption, its spectrum is thus expected not to change, but the head will stretch as we demonstrated in the experimental results presented here and to a much larger extend since the plasma length is 10 m. Later slices will interact in the nonlinear regime, they will also stretch in time and their spectrum will also broaden. Slices with intensities larger than the Rb ionization intensity will propagate in the plasma, with a much different dispersion relation ( $\chi_{pe} = -\omega_{pe}^2/\omega_0^2$ ). In particular the plasma has a dispersion that is much smaller than that of the vapor (at the same density) and very weakly dependent on frequency. They will therefore propagate essentially without either stretching in time or spectral broadening. These slices will be able to ionize the Rb over long distances. We therefore expect that the anomalous dispersion within the ionizing laser pulse arising from the Rb D2 (and to some lesser extend D1) line will not prevent the propagation of the core of the laser at intensities large enough to ionize the vapor over the expected 10 m. In addition, the population of Rb upper atomic states by the strong pumping from the laser pulse broad spectrum should lead to more effective ionization. Indeed, field ionization relies on direct ionization from the ground state. The intensity required for this ionization process scales with the fourth power of the ionization potential. Therefore, any electron promoted to an upper Rb atomic state by the laser pulse through the D2, D1 and other lines (see Figure 1) will be ionized at much lower laser intensities. The interaction of the laser pulse with the vapor is of course more complicated than outlined here. In particular, time evolution along the laser pulse, as well and radial intensity variations must be included. We are therefore studying these effects with 2D numerical simulations and we perform corresponding experiments.

# V. Conclusion

We studied experimentally the effect of (linear) anomalous dispersion around the D2 and D1 lines of a Rb vapor on the propagation of a low-intensity short laser pulse. Experimental results are in good agreement with a simple 1D calculation and with the results of a 2D model that will be used to describe the propagation of a high intensity laser pulse that will be used to ionize the Rb vapor for the AWAKE experiment.

### REFERENCES

[1] A. Caldwell, E. Gschwendtner, K. Lotov, P. Muggli, and M. Wing. (2013).

- AWAKE Design Report: A Proton-Driven Plasma Wakefield Acceleration Experiment at CERN. *CERN-SPSC-2013-013*; *SPSC-TDR-003*, 441 47 189.
- [2] P. Muggli, A. Caldwell, O. Reimann, E. Öz, R. Tarkeshian, C. Bracco, E. Gschwendtner, A. Pardons, K. Lotov, A. Pukhov, et al. (2013). Physics of the awake project. *TUPEA008, The proceedings of IPAC 2013*.
- [3] P. Bejot. (2009). Filamentation in gases: Master equations. , Universite de Bourgogne, BP 47870, 21078 Dijon Cedex, France.
- [4] P. Bejot. (2009). Theoretical and experimental investigations of ultra short laser filamentation in gases. University of Geneva, France.
- [5] E. Sansonetti. (2006). Wavelengths, Transition Probabilities, and Energy Levels for the Spectra of Rubidium (RbI through

- RbXXXVII) . Phys. Chem. Ref. Data, Vol. 35, No. 1.
- [6] Robert W. Boyd. (2008). Nonliear optics. *Elsevier*.
- [7] E. Öz, P. Muggli. (2014). A novel Rb vapor plasma source for plasma Wakefield accelerators. Nuclear Instruments and Methods in Physics Research A, 740 197 202.
- [8] S. V. Popruzhenko. (2014). Keldysh theory of strong field ionization: history, applications, difficulties and perspectives. *J. Phys. B: At. Mol. Opt. Phys*, 47 204001 (35pp).
- [9] A. Couairona, A. Mysyrowicz. (2007). Femtosecond filamentation in transparent media. *Physics Reports*, 441 47 189.
- [10] V. S. Popov. (2004). Tunnel and multiphoton ionization of atoms and ions in a strong laser field (Keldysh theory). *Physics-Uspekhi*, 47.9: 855.